Optical contamination screening of materials with a high-finesse Fabry-Perot cavity resonated continuously at 1.06-μm wavelength in vacuum

Daqun Li, Dennis Coyne, and Jordan Camp

An optical-loss measurement system based on a resonant Fabry–Perot cavity at 1.06 μm in vacuum has been developed for independent monitoring of the cavity total loss and the optical absorption loss. Maintenance of cavity resonance over a one-month period allows the assessment of long-term degradation of the cavity optics in the presence of outgassing materials, with sensitivities of 5 ppm/yr for total cavity loss and 2 ppm/yr for cavity absorption loss. Test results for light-emitting diodes, Kapton-insulated cable assemblies, and Vac-seal epoxy adhesive are given. Scaling of these results to the optical performance requirements of LIGO is discussed. © 1999 Optical Society of America

OCIS codes: 290.4210, 300.1030, 050.2230, 000.2780, 140.0140.

1. Introduction

The Laser Interferometer Gravitational-Wave Observatory (LIGO) project[1] uses high-power optical interferometry (~20 kW in the arm cavities, and ~300 W in the recycling cavity) to provide the required shot-noise-limited sensitivity for gravitational-wave detection. To achieve this goal, low-absorption optics must be used to avoid thermal effects, and scatter must be controlled to maintain optical efficiency and to avoid coupling to mechanical noise sources by means of multiple scattering. In addition to establishing the optics fabrication requirements, subsequent contamination of the optics (which are operated under high vacuum) must also be limited. Deposition on the coated surfaces of the optics from vacuum system contaminants can increase coating microroughness and subsequently cause light scattering, thereby reducing the available optical circulating power. Deposited contaminants, when illuminated with high-power optical beams, can also give rise to local heating owing to optical absorption. The heating can deform the optical figure or induce a thermal-lensing effect from the coupling of the thermal dependence of the refractive index to a temperature gradient in the affected optics.

To avoid these problems, LIGO has set a limit on the rate of increase in loss for its optics of no more than 10 ppm/yr scatter and 2 ppm/yr absorption. Representative samples of each material included in LIGO's vacuum system must be screened to ensure the material does not induce optical losses exceeding the LIGO loss limit. As a wide variety of materials are used in large amounts and the consequences of surface contamination are not readily amenable to theoretical prediction, contamination screening of materials has to be conducted experimentally. It has been demonstrated that total mirror losses can be inferred with a resolution of 5 ppm by measurement of the power storage time of an optical cavity composed of the mirrors to be tested.[2] This technique led to an initial investigation at LIGO to study the contamination effects of Fluorel and RTV-615 springs on 110-ppm nominal transmission mirrors at a wavelength of 515 nm.[3] The study reported here was undertaken, as additional data were needed for a larger range of materials and at the built design wavelength of LIGO (1064 nm).

The loss measurement based on optical cavity storage time can only imply the total cavity loss, that is, the sum of mirror transmission, scatter, and absorption losses. It cannot, however, distinguish the absorption loss from the total cavity loss as required by LIGO. There are a number of techniques such as photoacoustic sensing[4] and photothermal detection[5,6] capable of measuring surface absorption down to the

The authors are with the Laser Interferometer Gravitational-Wave Observatory Project, California Institute of Technology, MS 18-34, Pasadena, California 91125. J. Camp's e-mail address is jordan@ligo.caltech.edu.

Received 29 March 1999.
0003-6935/99/255378-06$15.00/0

parts per million level; however, none of these techniques can be readily applied to a resonant optical cavity under vacuum. We have chosen an optical absorption loss measurement that is implemented in a resonant optical cavity by evaluation of the shift in beat frequency of two transverse electromagnetic (TEM) modes resonated simultaneously in the cavity.[7] The shift occurs because the curvature deformation of cavity mirrors caused by heating due to optical absorption changes the cavity optical geometry and consequently alters the frequency spacing of the cavity resonant modes.

In this paper we describe an optical-loss measurement system in which the cavity storage-time-based loss measurement and the absorption-loss detection are adapted to one system. The implementation of two independent loss measurements in one system also allows results to be cross checked under the same condition. The capability of maintaining our optical cavity on resonance continuously over long periods allows us to examine the effect of the laser field on the possible intensity-dependent dissociation and surface deposition of gaseous contaminants. Thus the system provides a powerful tool for evaluating the long-term optical contamination pattern of materials. So far we have used the above two independent loss-detection techniques to conduct contamination studies of LIGO materials such as epoxy-encapsulated light-emitting diodes (LED's), Kapton cable assemblies, and Vac-seal epoxy adhesive. Scaling of the testing results to LIGO is also discussed in this paper.

2. Loss-Measurement Principles and Modeling

A. Total Cavity Loss

If a laser beam is injected into a high-finesse Fabry–Perot cavity composed of low-loss mirrors and the laser frequency is stabilized to one of the cavity modes with a good optical coupling efficiency, the intracavity optical circulating power begins to build until it reaches a steady power level. Conversely, if a resonant optical cavity at a steady state is shut off, the stored optical power in the cavity displays a characteristic decay as

$$I_t(t) = I_t(0)\exp(-t/\tau), \tag{1}$$

where $I_t(t)$ is the transmitted power from the cavity at time t counting from the shutoff moment, $I_t(0)$ is the cavity transmitted power initially at the shutoff moment, and τ is the cavity power storage time, also called cavity power decay time. The cavity power storage time in relation to the total cavity loss can be expressed by

$$L_{\text{loss}} = 2l/c\tau, \tag{2}$$

where l is the cavity mirror separation and c is the speed of light. The total cavity loss represents the sum of cavity transmission, scatter, and absorption losses.

B. Cavity Optical Absorption Loss

The surface optical absorption of optics can be inferred from thermal expansion of the heated optic surfaces with the optics configured to form a resonant optical cavity. The absorption-induced surface expansion of cavity mirrors changes the optical geometry of the cavity and therefore alters the frequency spacing between cavity modes. To a first approximation, the surface thermal expansion of an optic under optical illumination can be expressed by a change in the sagitta as[8]

$$\delta s \approx (\alpha/4\pi\kappa)P_a, \tag{3}$$

with α the thermal expansion coefficient, κ the heat conductivity of the substrate, and P_a the absorbed optical power. For simplicity, in the case of a flat mirror, the sagitta change can be interpreted as a radius of curvature change of the heated optic of

$$R_{\text{eff}} = w^2/2\delta_s, \tag{4}$$

with w the beam waist on the optic surface, thus altering the cavity g factor as,

$$g' = 1 - l/R_{\text{eff}} = 1 + 2l\delta s/w^2. \tag{5}$$

Given that the stored power of a resonant cavity P_s is the ratio of the cavity output power I_t to the cavity output mirror transmissivity T, one can rewrite Eq. (5) as

$$g' = 1 + \alpha l I_t A/2\pi\kappa w^2 T, \tag{6}$$

knowing that

$$P_a = P_s A, \tag{7}$$

where A is the surface optical absorbance of the heated optic. Since the frequency spacing between two cavity modes of different order is a function of cavity g factors, surface optical absorbance of cavity mirrors can be inferred by measurement of the shift in such frequency spacing at two cavity-illuminating power levels accordingly[9] as

$$(\Delta\nu_{10-00})' - (\Delta\nu_{10-00})'' = \frac{c}{2\pi l}\cos^{-1}\{[(g_1)'(g_2)']\}^{1/2} - \frac{c}{2\pi l}\cos^{-1}\{[(g_1)''(g_2)'']^{1/3}\}, \tag{8}$$

with subscripts 10 and 00 representing a first-order mode and its adjacent fundamental mode, subscripts 1 and 2 referring to mirrors 1 and 2 supposing a two-mirror cavity, and single and double primes indicating two different illuminating power levels. For our test apparatus, we use a flat-concave (1-m radius) cavity composed of 65-ppm transmission fused-silica mirrors ($\alpha/\kappa = 3.3 \times 10^{-7}$ m/W) with a mirror separation of 0.5 m. A 400-W change in cavity stored power with 1 ppm total cavity absorption shifts the beat frequency between a TEM_{00} mode and its adjacent first-order mode of the cavity by ~3 kHz

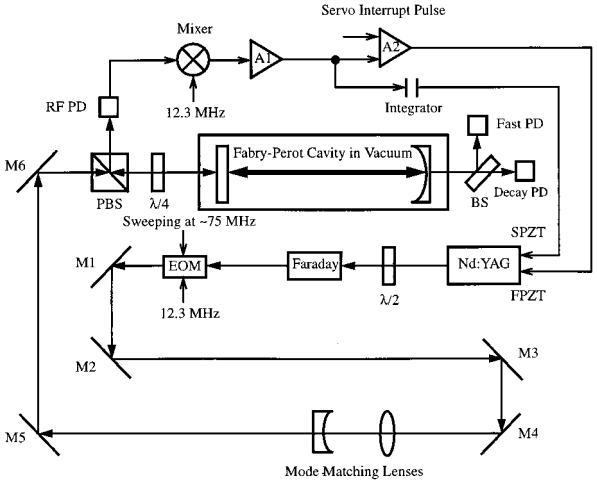

Fig. 1. Schematic diagram of the optical contamination cavity setup. $\lambda/2$ and $\lambda/4$, half-wave and quarter-wave plates; M1–M6, mirrors; EOM, electro-optic modulator; PBS, polarizing beam splitter; PD, photodetector; A1 and A2, low-noise amplifiers; BS, beam splitter; SPZT and FPZT, slow and fast piezofrequency actuators of the laser frequency servo system. The PBS in combination with the $\lambda/4$ plate function to discriminate the cavity reflection beam from the incident beam. The decay PD is used to monitor the cavity transmitted power decay for total cavity loss measurement, whereas the fast PD measures the beat frequency between cavity resonant modes for optical absorption inference.

out of an initial separation of roughly 75 MHz, according to the above equations.

We have developed a finite-element code to model the surface deformation caused by heating with a Gaussian laser spot. We found agreement at the 20% level with the estimates above.

3. Apparatus and Experimental Procedures

The basic apparatus for our experiments is a two-mirror Fabry–Perot cavity in a vacuum chamber kept on resonance continuously by our locking the frequency of a source Nd:YAG laser (Lightwave Electronics, 126) to one of the cavity's TEM_{00} modes, as shown schematically in Fig. 1. The cavity was composed of both a flat and a concave mirror with a radius of curvature of 1 m. We separated the two mirrors by 0.5 m, which yielded a beam waist of 0.4 mm, by attaching them to each end of a hollow cylindrical glass spacer with side holes for vacuum venting. The spacer was suspended with thin metal wires for vibration isolation. The fused-silica mirrors were coated to have normal transmissivity of $\sim$65 ppm at 1064 nm. The cavity chamber of $\sim$20 800 cm^3 in volume was pumped continuously with an ion pump (Varian, 921-2001) at a pumping speed of 8 1/s to maintain the vacuum at $\sim 10^{-6}$ Torr. The laser was locked to the cavity resonance with the radio frequency (RF) phase-modulated reflection technique.[10] The laser beam was phase modulated at 12.3 MHz with an electro-optic modulator (New Focus, 4004). Light returning from the cavity input coupler was detected by a RF photodetector with its photocurrent multiplied against the modulating RF waveform in a double-balanced mixer. The mixed signal was integrated to form a bipolar error signal that indicated the magnitude and sign of the laser frequency's deviation from the cavity eigenfrequency. This signal was filtered and fed back to the laser's frequency control input to maintain cavity resonance. With the aid of a pair of mode-matching lenses, at least 80% of incident light was coupled into a cavity's TEM_{00} mode.

We measured the decay time of our resonant cavity by transitorily disabling the cavity resonance with a transient pulse signal (200 μs wide) sent to interrupt the frequency servo electronics, while monitoring the cavity transmitted power decay via a photodetector with the aid of a digital storage oscilloscope. A wide-frequency bandwidth (100 kHz) photodetector was employed for accurate measurement of the transmitted power decay of our cavity, typically near 24 μs. It was found that the cavity decay time varies with a varying temperature in the surrounding environment, possibly owing to a relative position change between the two cavity mirrors, as induced by temperature variations. To minimize this problem, the cavity chamber was temperature stabilized within 0.5 K at a temperature set a few degrees Celsius above ambient temperature. Typically, 100 mW of laser power was incident onto our cavity with $\sim$700-W optical power stored in the cavity, leading to $\sim$150 kW/cm^2 in stored power density, comparable with that used in the highest-intensity cavities (the mode-cleaner cavities) in LIGO.

To measure the beat frequency between cavity resonant modes for absorption inference, we generated additional sidebands that we swept using the same electro-optic modulator with a RF signal generator (Hewlett Packard, 8656B/001) while keeping the cavity locked at a TEM_{00} mode. When the sidebands were swept across the beat frequency, we obtained the amplitude profile of the first-order mode resonated adjacently to the locked TEM_{00} mode by monitoring the cavity transmitted signal with a fast photodetector (New Focus, 1811) and then by demodulating the detector output at the RF frequency. We achieved continuous adjustment of incident laser power by rotating a half-wave plate located in front of a Faraday isolator, shown in Fig. 1, while still maintaining the cavity on resonance.

For an initially clean and stable environment for future material screening to be provided, the cavity interior chamber, including the glass spacer with the exception of cavity mirrors, was vacuum baked at 200 °C for three days. Subsequently, for one month total cavity loss and absorption loss of the empty clean cavity were monitored continuously from the resonant cavity to ensure the observed losses stayed low and stable. Next, test materials for screening were prepared according to LIGO procedures. The preparations generally involved a cleaning, a vacuum baking, and then a residual gas analysis scanning. The materials with an acceptable residual gas analysis scan were then carefully loaded into the cavity chamber or the glass spacer, if possible, so that they faced the

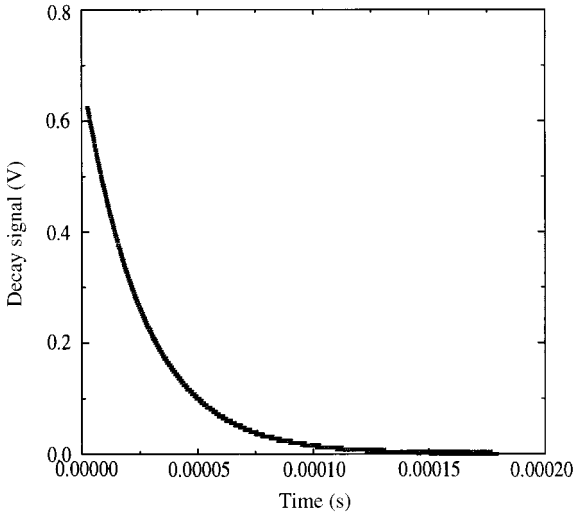

Fig. 2. Exponential decay in cavity stored power with a decay time of 25.738 ± 0.018 μs corresponding to 129.51 ± 0.09 ppm in total cavity loss. Multiplication symbols (×) represent the experimental data points and the solid curve is the least-squares-fitted exponential curve.

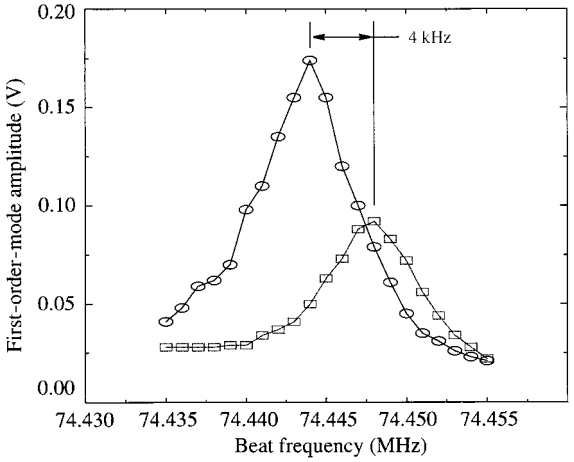

Fig. 3. Shift of a first-order mode frequency due to a 400-W change in cavity stored power with the cavity locked to a fundamental mode, revealing roughly 1.3 ± 0.4 ppm in cavity total absorption loss.

cavity mirrors as closely as possible. Total cavity loss and cavity absorption loss were independently monitored for one month, and annual cavity losses were extrapolated from the amassed data to compare with the LIGO loss limit. To date, three in-vacuum components or assemblies have been tested in our cavities. Five Toshiba LED's (TLN107A) and five Toshiba integrated circuit (IC) chips (TPS703A) were tested in one test cycle. The equivalent of 1440 bonds ($\sim 2 \times 10^{-4}$ cm^3 per bond) of Vac-seal epoxy (Physical Electronics, 288-6000) was spread (15 cm × 5 cm) onto a piece of clean aluminum foil and cured for 72 hrs before being loaded into the cavity in a second test. The LEDs and IC chips and the Vac-seal epoxy were loaded into the glass spacer of the cavity that viewed the cavity mirrors directly. In a third test, Kapton ribbon cables, with 25-pin, D-type connectors, all manufactured by MDC Vacuum Products, with a total surface area of ~200 cm^2, were placed outside the spacer but facing the side vent holes of the spacer for maximum mirror exposure.

4. Results and Discussion

A. Material Screening Results

The result of 128 averages of the power decay of a cavity TEM_{00} mode, fitted with an exponential function, is illustrated in Fig. 2. The fitted decay time (τ) of 25.738 ± 0.018 μs corresponds to 129.51 ± 0.09 ppm in total cavity loss according to Eq. (2). Also, from this decay time, the finesse of the cavity can be derived to be $\sim 4.84 \times 10^4$, from the ratio of the free spectral range of the cavity, 300 MHz, to the cavity intensity linewidth, 6.2 kHz.

A 4-kHz shift in beat frequency between a TEM_{00} mode and its adjacent first-order mode was observed from our cavity with respect to the ~400 W change in cavity stored power, as demonstrated in Fig. 3, indicating roughly 1.3 ± 0.4 ppm, including uncertainties from modeling and measurement errors, for cavity total absorption loss (summed surface absorption loss of cavity mirrors) as implied by Eqs. (3)–(8). In this figure, the higher- and lower-peak curves correspond to the amplitude profiles of a first-order mode at higher and lower illuminating power levels, respectively. The beat frequency was observed to shift toward the higher frequency at a lower stored power level, as anticipated theoretically by Eq. (8). The cavity beat frequency measurement requires multiple-cavity spatial-mode excitation, which we did by a slight mode misalignment. Apart from cavity misalignment, the amplitude of a first-order mode profile needs to be optimized by a defocusing of the cavity transmitted beam to overfill the active area of the detecting photodiode, as otherwise the detector would detect no beating between the orthogonal fundamental and the first-order modes. For detector saturation to be avoided, the optical power incident onto the detecting photodiode was typically attenuated not to exceed 5 mW.

Figure 4 shows the monitored cavity decay time (total cavity loss) and total absorption loss over 33 days for Vac-seal epoxy with the slopes least-squares fitted for both losses. The fitted slopes were used to predict the annual total or absorption loss change in our test apparatus. The measurement errors, typically near 0.02 μs, are too small to account for the 0.2-μs decay time fluctuations displayed in Fig. 4. These fluctuations can be partially explained by the residual temperature drift of the cavity chamber near 0.5 K, because, without temperature stabilization of the cavity chamber, the decay time of this cavity was found to fluctuate with room temperature at ~0.3 μs/K. These fluctuations were most likely caused by relative position change between cavity mirrors during the measurement period, since the cavity decay time measured with a first-order mode deviated

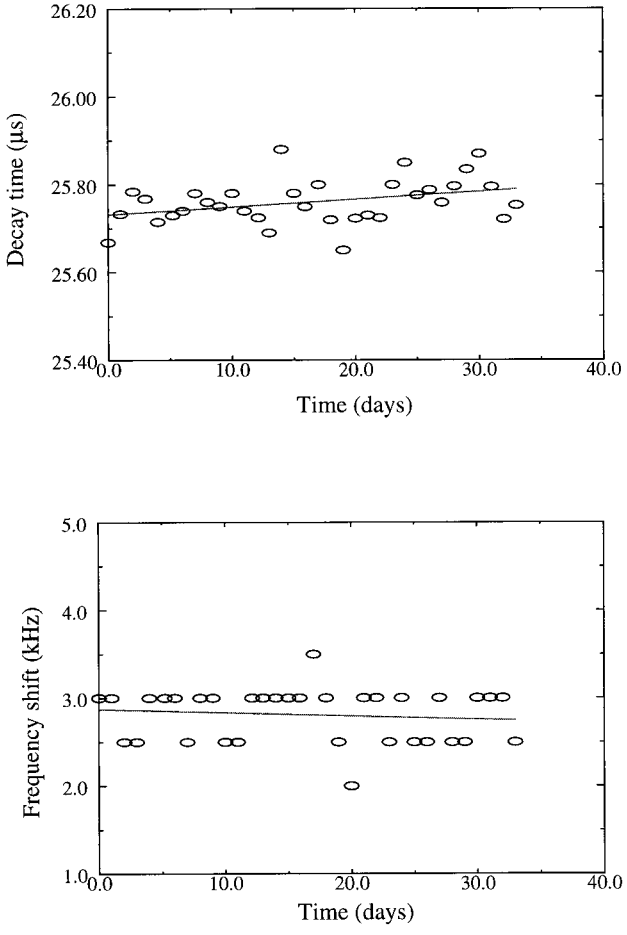

Fig. 4. Decay time (top trace) and shift of the first-order mode frequency (bottom trace) with a consistent step change in cavity stored power for the cavity containing Vac-seal epoxy over 33 days. Linear least-squares fit of the data against time yields slopes of $+0.005 \pm 0.001$ μs/day for the decay time and -0.004 ± 0.005 kHz/day for the frequency shift.

from that measured with a fundamental mode by 0.4 μs (~2 ppm change in total cavity loss), indicating that the mirror reflectivity is not perfectly uniform over the coating surface. Table 1 summarizes the testing results of the LED's and IC chips, the Kapton-insulated cable assemblies, and the Vac-seal epoxy for the two-mirror cavity. The data for LED's were obtained initially when the cavity chamber was not temperature stabilized; thus the annual scatter and absorption loss of 8.54 ppm may result in part from the temperature effect on the decay time measurements as stated above. For other materials in this table, no significant loss trends can be seen except for Kapton cables, which implies an annual increase of 8.43 ± 2.14 ppm in scatter and in absorption losses. Because a stable absorption loss was monitored over the same period, the above loss increase may solely result from scatter loss. It can be also concluded that our system has an annual sensitivity of ~5 ppm in total cavity loss and ~1 ppm in total absorption loss. Note that the above material losses were derived in our test apparatus. In the real environment of LIGO, the above losses must be scaled down drastically owing to the higher vacuum pumping speed and the larger chamber volume existing in LIGO (see the following analysis).

B. Scaling of Results to LIGO

The most straightforward model of optical contamination assumes that loss is caused by volatile materials that break through interaction with the laser beam and adhere to the optic surface. Thus the scaling of optical-loss rates from our measurement apparatus to the LIGO optics depends on the light intensity and the contaminant flux at the optic for the two environments. As the intensity in our tests was at the highest level planned in the LIGO cavities (150 kW/cm^2), we can assume that the optical degradation will scale no worse than the contaminant flux. The flux has a direct, line-of-sight component between the outgassing material and the optic surface and an indirect component involving the equilibrium partial pressure of the contaminant species. The fluxes are given by

$$\Phi_D = \frac{3.3 \times 10^{19} J}{4\pi r^2}, \tag{9}$$

$$\Phi_P = \frac{P}{(2\pi MkT)^{1/2}} = \frac{2 \times 10^{21} P}{(AMU)^{1/2}}, \tag{10}$$

where Φ_D and Φ_P are the direct and the indirect fluxes in molecules per second per square centimeters, J is the outgassing rate in torr-liter per second, r is the distance from the material to the optic, P is the partial pressure, M is the molecular mass, k is the Boltzmann constant, T is the absolute temperature, and AMU is the atomic mass number of the outgassed species.[11] P is given by

$$P = J/S_{\text{tot}}, \tag{11}$$

where S_{tot} is the total pumping speed, which may include pumping provided by the clean vacuum chamber walls: $S_{\text{tot}} = S_{\text{pump}} + S_{\text{chamber}}$. The amount of material tested in the contamination test apparatus was roughly the same as that planned for use in LIGO chambers (for most materials tested), so that J is approximately the same for both environments. Ignor-

Table 1. Annual Loss Predictions of LED's and IC Chips, Kapton Cable Assemblies, and Vac-seal Epoxy Adhesive in Contamination Test Apparatus

Measured Loss (ppm)	LED's and IC Chips[a]	Kapton Cable Assemblies	Vac-seal Epoxy Adhesive
Annual scatter and absorption loss	$+8.54 \pm 2.64$	$+8.43 \pm 2.14$	-3.88 ± 1.94
Annual absorption loss	$+0.7 \pm 0.5$	-1.3 ± 0.7	-0.5 ± 0.6

[a]Data were obtained before temperature stabilization of cavity chamber was introduced.

ing pumping by gettering of the vacuum chamber walls and using the respective LIGO and test cavity pumping speeds of 3000 and 8 1/s, we find the fluxes of Eqs. (9) and (10) become equal for $AMU = 500$ at separations of 5 and 0.3 cm. These numbers are smaller than the material-to-optic separation in either LIGO or the test cavity. Thus we can generally ignore the line-of-sight flux for point sources, though this term can be significant for larger, distributed sources. The flux, and therefore the loss rate, is seen to scale inversely with the pumping speed, or approximately 400 times lower in LIGO than in the test cavity. Finally, the LIGO vacuum chamber has a surface area of 1.6×10^7 cm^2, while the contamination test chamber has an area of 2.1×10^4 cm^2. Thus we may assume that hydrocarbon pumping by the clean chamber surface is likely to be of the same order of ratio as that for the commercial pumps. This implies that the test results give an extremely conservative estimate of the optical losses expected in LIGO.

We thank our colleagues in the LIGO project, especially Stan Whitcomb and Albert Lazzarini, for their useful suggestions in conducting this research. We also thank David Shoemaker and Mike Zucker for their assistance in preparing this manuscript. The National Science Foundation is acknowledged for their financial support of this research (PHY-9210038).

References

1. A. Abramovici, W. E. Althouse, R. W. P. Drever, Y. Gürsel, S. Kawamura, F. J. Raab, D. Shoemaker, L. Sievers, R. E. Spero, K. S. Thorne, R. E. Vogt, R. Weiss, S. E. Whitcomb, and M. E. Zucker, "LIGO: the laser interferometer gravitational-wave observatory," Science **256,** 325–333 (1992).
2. D. Z. Anderson, J. C. Frisch, and C. S. Masser, "Mirror reflectometer based on optical cavity decay time," Appl. Opt. **23,** 1238–1245 (1984).
3. A. Abramovici, T. T. Lyons, and F. J. Raab, "Measured limits to contamination of optical surfaces by elastomers in vacuum," Appl. Opt. **34,** 183–185 (1995).
4. A. C. Tam, "Applications of photoacoustic sensing techniques," Rev. Mod. Phys. **58,** 381–431 (1986).
5. E. Welsch and D. Ristau, "Photothermal measurements on optical thin films," Appl. Opt. **34,** 7239–7253 (1995).
6. Z. L. Wu, M. Thomsen, P. K. Kuo, Y. S. Lu, C. Stolz, and M. Kozlowski, "Photothermal characterization of optical thin film coatings," Opt. Eng. **36,** 251–262 (1997).
7. N. Uehara, E. K. Gustafson, M. M. Fejer, and R. L. Byer, "Modeling of efficient mode-matching and thermal-lensing effect on a laser-beam coupling into a mode-cleaner cavity," in *Modeling and Simulation of High-Power Laser Systems IV*, U. O. Farrukh and S. Basu, eds., Proc. SPIE **2989,** 57–68 (1997).
8. W. Winkler, K. Danzmann, A. Rüdiger, and R. Schilling, "Heating by optical absorption and the performance of interferometric gravitational-wave detectors," Phys. Rev. A **44,** 7022–7036 (1991).
9. P. W. Milonni and J. H. Eberly, *Lasers* (Wiley, 1988), p. 505.
10. R. W. P. Drever, J. L. Hall, F. V. Kowalski, J. Hough, G. M. Ford, A. J. Munley, and H. Ward, "Laser phase and frequency stabilization using an optical resonator," Appl. Phys. B **31,** 97–105 (1983).
11. J. F. O'Hanlon, *A User's Guide to Vacuum Technology* (Wiley, 1989), pp. 8–23.